Indonesian Journal of Pharmacy

VOL 36 (4) 2025: 622–637 | RESEARCH ARTICLE

Formulation and Evaluation of Moringa Seed Oil Nanoemulsion Using Polyoxyl 40 Hydrogenated Castor Oil and Glycerin as a Surfactant-Cosurfactant System

Uswatun Chasanah[1,2], Nining Sugihartini[3*] and Sapto Yuliani[3]

1. Doctoral Programme in Pharmacy Science, Faculty of Pharmacy, Universitas Ahmad Dahlan, Jl. Prof. DR. Soepomo, Yogyakarta, 55164, Indonesia
2. Department of Pharmacy, Faculty of Health Science, Universitas Muhammadiyah Malang, Malang, 65145, Indonesia
3. Faculty of Pharmacy, Universitas Ahmad Dahlan, Jl. Prof. DR. Soepomo, Yogyakarta, 55164, Indonesia

Article Info

Submitted: 09-12-2023
Revised: 14-03-2025
Accepted: 14-3-2025

*Corresponding author
Nining Sugihartini

Email:
nining.sugihartini@pharm.uad.ac.id

ABSTRACT

Moringa seed oil has antioxidant and anti-inflammatory activities, but these activities have yet to produce an optimal outcome due to the moringa seed oil's low skin penetration ability, leading to the need for moringa seed oil formulation into nanoemulsion preparations. This study aimed to develop a moringa seed oil nanoemulsion using PEG-40 hydrogenated castor oil as a surfactant and glycerin as a cosurfactant. Studies of pseudo-ternary phase diagrams show that the surfactant-cosurfactant (S-mix) ratio of 1:1 is the most optimal, resulting in the broadest area of nanoemulsions. In this study, six formulas of moringa seed oil nanoemulsion were developed with 5–7% oil concentrations. Characterization showed that the sizes of the nanoemulsion globules ranged from 22.33 to 40.02 nm, with a polydispersity index (PDI) ≤ 0.2, indicating a uniform particle distribution. The zeta potential values ranged from -13.73 to -22.57 mV, indicating moderate stability. The moringa seed oil nanoemulsion formulas maintained stable pH (6.7–7.3) during storage and thermal stability tests, suitable for topical applications. The high percent transmittance (≥94%) confirmed transparency, while the antioxidant activity was significantly increased compared to pure oils. The study results show that the nanoemulsion formula with the composition of moringa seed oil, S-mix, and water in the ratio of 5:55:40 with an S-mix ratio of 1:1 was the most physically and chemically stable and was high in bioactivity potential. This research encourages the use of nanoemulsion technology to improve the effectiveness of natural active ingredients in topical formulations.

Keywords: Antioxidants, topical formulations, characteristics, stability

INTRODUCTION

Moringa (*Moringa oleifera*) seed oil is widely known for its various pharmacological benefits (Shahbaz et al., 2024). Moringa seed oil (MSO) primarily contains essential fatty acids, especially oleic acid, with a content of 73.36% (Gharsallah et al., 2021). Oleic acid has activities as a moisturizer (Alander, 2012) and anti-inflammatory (Santa-María et al., 2023; Santamarina et al., 2021). In addition, in moringa oil, there are sterols, especially beta-sitosterol, which also have activities as an anti-inflammatory and antioxidant (Zhang et al., 2023). Other contents of moringa oil, such as tocopherols, especially α-tocopherols, and phenol compounds, are active as antioxidants (Leone et al., 2016). Previous study results show that oleic acid at a concentration of 3% already provides anti-inflammatory effects (Pegoraro et al., 2021). The various active compounds in MSO result in high potential of MSO for topical applications as an anti-inflammatory and antioxidant (Santa-María et al., 2023; Santamarina et al., 2021; Shahbaz et al., 2024; Zhang et al., 2023), moisturizer (Purnamawati et al., 2017), and anti-wrinkle (Kleiman et al., 2008) and for faster healing of skin wounds (Ventura et al., 2021).

MSO exhibits low solubility in aqueous systems due to its hydrophobic nature, and direct application of MSO on the skin has a limited skin penetration ability. This limitation can be overcome using a nanoemulsion delivery system. Research has taken considerable interest in nanoemulsions' extensive applications as drug and active ingredient delivery technologies due to their small droplet size (typically < 100 nm), which provides advantages such as better physical stability, increased skin penetration, and higher bioavailability compared to conventional formulations (Gupta et al., 2016). Nanoemulsions also offer advantages over liposomes, microparticles, solid lipid nanoparticles (SLN), and nanostructured lipid carriers (NLC) by preventing coalescence, improving absorption, and enabling easier large-scale manufacturing (Aditya et al., 2014; Wu et al., 2022). The success of nanoemulsion formulations depends on the selection of surfactant and cosurfactant to use. The surfactant and cosurfactant combination determines the system's stability and the efficiency of the dispersed active ingredients (Gaikwad et al., 2024). Previous research has shed light on the use of various surfactants, such as Tween 80, Span 80, or whey protein, in the formulation of MSO nanoemulsions (Abdelraouf et al., 2023; Nita et al., 2019). Although MSO produces good nanoemulsions, a decrease in stability during storage under certain conditions has been reported (Abdelraouf et al., 2023; Nita et al., 2019). As such, it is deemed necessary to find surfactants and cosurfactants that can provide good stability in the formulation of MSO nanoemulsions.

To date, no research has utilized polyoxyl 40 hydrogenated castor oil (PEG-40 HCO) as a surfactant and glycerin as a cosurfactant in formulating MSO nanoemulsions. This combination has reportedly been effective in producing nanoemulsions using other active ingredients (Winarti et al., 2021; Xiao et al., 2013). The advantage of PEG-40 HCO over other surfactants comes not only from its ability to form stable nanoemulsions but also from the safety level that it offers when used at high concentrations in formulations (Rachmawati et al., 2017). PEG-40 HCO with HLB 14-16 can dissolve fatty acids, which are the main ingredients of MSO (Rowe et al., 2009). Therefore, it is considered highly suitable to use in forming MSO nanoemulsions as oil nanoemulsions in water. Meanwhile, as a cosurfactant, glycerin helps increase the interface's fluidity, which increases the surfactant's ability to form nanoemulsions. In addition, glycerin is non-toxic, can increase viscosity, has enhancer properties, and is resistant to oxidation (Nadya et al., 2020; Rowe et al., 2009). Therefore, the combination of PEG-40 HCO and glycerin was chosen in this study because it can produce good physical stability and boosts safety to use, compatibility with natural active ingredients, and potential to increase the penetration and bioavailability of active ingredients. This study aimed to fill this gap by developing an MSO nanoemulsion formulation using PEG-40 HCO and glycerin as a surfactant-cosurfactant system. In addition, this study also evaluated the antioxidant activities of the nanoemulsions produced to demonstrate the functional benefits of the combination formulations used. The novelty of this research lies in its use of a combination of PEG-40 HCO and glycerin in the formulation of MSO nanoemulsions. To the author's knowledge, this has never been researched, so this study is expected to make a new contribution to the advancement of nanoemulsion technology using natural active ingredients.

MATERIALS AND METHODS

The ingredients used in this research were moringa seed oil obtained from PT Moringa Indonesia Fangardana, Indonesia, PEG-40 HCO (Emulsogen®HCO40, Clariant), glycerin (ex-Wilmar, Indonesia), deionized water (Waterone OneMed), methanol (Merck, Germany), and 2,2-diphenyl-1-picrylhydrazyl (DPPH) (Merck, Germany). The instruments used in the research were a digital hotplate stirrer (RIO), homogenizer (Heidolph RZR 2021), transmission electron microscope (TEM Jeol JEM 1400 120 kV), FTIR spectrophotometer (IRSpirit/ATR-S Serial No. A224158/Shimadzu), cone and plate viscometer (Rheosys Merlin VR II), climate chamber (Climacell and Memmert), viscometer (Brookfield), spectrophotometer (UVmini-1240, Shimadzu-Japan), particle size analyzer/zetasizer (Malvern Instrument), pH digital meter (SI Analytics Lab 845), centrifuge (Nuve, NF200), and CHEMIX School software.

Making Pseudo-ternary Phase Diagrams

The making of pseudo-ternary phase diagrams involved finding the concentration ranges of the components that made up the nanoemulsions using the water titration method. Three ratios of PEG-40 HCO as surfactant (S) to glycerin as cosurfactant (CoS), expressed as S-mix, were used, i.e., 3:2, 1:1, and 2:3 (w/w). The

following MSO:S-mix ratios were used: 1:12, 1:11, 1:10, 1:9; 1:8, 1:7: 1:6, 1:5, 2:8, 3:7, 4:6, 5:5, 6:4,7:3, 8:2, and 9:1. Comparisons were carried out following previous research by Kiromah et al. (2023) with some modifications. The mixture of MSO and S-mix was stirred using a magnetic stirrer at a speed of 500 rpm until homogeneity was achieved at a temperature of 60° C, which took 60 minutes. The MSO and S-mix mixture was then slowly titrated with deionized water. The titration endpoint was the point at which the solution became cloudy. The number of water phases required to produce a turbid mixture was noted. The sample was classified as a nanoemulsion when it appeared as a clear liquid (Gradzielski et al., 2021). The nanoemulsion region was identified as a mixture of transparent and isotropic liquids. Each percentage value or mixed part—oil and S-mix, or water and S-mix, or oil and water—was fed into the CHEMIX School software to obtain a pseudo-ternary phase diagram (Vibhute et al., 2015).

Moringa seed oil nanoemulsion (NE-MO) formulations

Based on the pseudo-ternary phase diagrams that were created, six formulations of moringa seed oil nanoemulsion (NE-MO) were developed, each measuring 100 g. MSO and S-mix were initially put in a glass beaker and mixed using a homogenizer at 1000 rpm at 60–70° C for 60 minutes. Purified water in an appropriate amount was gradually added to the mixture. The final mixture was stirred at a constant stirring speed (1000 rpm) for 10 minutes until a NE-MO was formed. This method was adopted from Nita et al. (2019) with slight modifications.

Evaluation of NE-MO

Droplet size and polydispersity index (PDI) determination

The average globule size and the nanoemulsion polydispersity index (PDI) were determined using a particle size analyzer (Malvern Panalytical). Samples were prepared by dissolving 100 μL of NE-MO in purified water to obtain a volume of 10 mL (100 dilutions). Each sample was then inserted into a transparent cuvette 1 cm^3 in volume in a thermostatic chamber at 25° C. The laser light scattering was monitored at a fixed angle of 90°. The measurement was repeated three times.

Zeta potential measurement.

The surface charge of the nanoemulsions was measured using a zetasizer (Malvern Panalytical Zetasizer). Measurements were carried out three times. Each NE-MO sample was diluted 100 times in 10 mL of deionized water, and then 375 μL of the dilution result was put into a cuvette, which was in turn put into a device for measurement.

Morphological study

The nanoemulsions' morphology was determined using a transmission electron microscope (TEM Jeol JEM 1400 120 kV). The nanoemulsions were mixed with deionized water (50 μL in 2.0m L) and then dripped at 10 μL over specimens. A 400-mesh grid tool was placed on top of each specimen with a droplet of nanoemulsion preparation and left for one minute. The remaining droplets of the preparation on the grid were cleaned using filter paper. Then, a drop of 10 μL of 2% uranyl acetate was placed on the grid, and the remaining drops were cleaned using filter paper. The grid was left for 30 minutes to dry, and then the image was visualized with TEM at a 100-kV acceleration voltage.

Drug–excipient interaction study

Molecular interactions between MSO and excipients were examined using Attenuated Total Reflectance Fourier Transform InfraRed (ATR-FTIR) spectroscopy (IRSpirit/ATR-S Serial No. A224158/Shimadzu). ATR-FTIR measurements were performed at room temperature (25° C). The constituent materials of NE-MO—MSO, PEG-40 HCO, and glycerin—and their mixtures were analyzed. The materials examined were dripped on the surface of the ATR crystal and scanned at a wave number of 4000 to 400 cm^{-1} in the FTIR instrument. In addition, a spectral analysis was performed.

pH test

pH measurement was carried out using a pH meter (SI Analytics Lab 845), calibrated using a phosphate buffer solution, with pH set at pH 4 and 6.86 (two-point calibration). The electrode was immersed in each sample until a constant number was obtained at room temperature (25° C). The measurement was carried out in triplicate.

Viscosity measurement

The viscosity of the NE-MO was measured at 25° C with a cone/plate 2.0/30-mm viscometer (Rheosys). Each measurement was performed in triplicate.

Percent transmittance test

NE-MO transparency was determined by measuring the percent transmittance at 650 nm using a UV-Vis spectrophotometer (UVmini-1240, Shimadzu, Japan) with distilled water as a blank. Good nanoemulsions show a percent transmittance

of more than 90% (Rosyidah et al., 2024). The measurement was carried out in triplicate.

Physical stability study

Centrifugation

Centrifugation tests were carried out before and after a heating-cooling cycle stability test. Each sample was placed in a tube and centrifuged at 5000 rpm for 30 minutes. The NE-MO formulas' onset of turbidity or phase separation was observed visually (Azeem et al., 2009).

Heating-cooling cycle stability study

The NE-MO formulas were stored at 4° C for 24 hours and then transferred to 40° C for 24 hours (1 cycle). The test was carried out in six cycles (Tunit et al., 2022).

Antioxidant activity

A NE-MO antioxidant activity test was carried out using 2,2-diphenyl-1-picrylhydrazyl (DPPH). This test began with the determination of the IC50 of MSO. In this test, vitamin C was used as a control. Each NE-MO sample was tested by adding 2 g of NE-MO sample to 2 mL of DPPH solution (0.4 mM), after which methanol was added to 10 mL. The solution was incubated at 37° C for 30 minutes and then centrifuged at 10,000 rpm for 60 minutes. The absorption of the filtrate was measured at a wavelength of 517 nm using a UV spectrophotometer (UVmini-1240, Shimadzu-Japan) (Chasanah, 2021).

Statistical Analysis

Results are expressed as mean±SD, and the minimal significance level was considered at $p < 0.05$. All statistical analyses were assessed using SPSS Version 26.0. Different groups were tested using a parametric paired t-test and one-way analysis of variance (ANOVA) with Tukey's HSD.

RESULTS AND DISCUSSION

Pseudo-ternary phase diagram study

A pseudo-ternary phase diagram determines the nanoemulsion region's oil, surfactant, and cosurfactant ratio. Pseudo-ternary phase diagrams can estimate the appropriate proportions of the water phase, oil phase, and surfactant concentration (Wang et al., 2017). Pseudo-ternary phase diagrams of formulas that used different S-mix ratios 3:2, 1:1, and 2:3 (Figure 1). The pseudo-ternary phase diagram of the MSO nanoemulsion formula with an S-mix ratio of 3:2 had a narrower area of that of the MSO nanoemulsion formula with an S-mix ratio of 1:1. The concentration of PEG-40 HCO as the dominant surfactant in the nanoemulsion formula with the S-Mix ratio of 3:2 led to the formation of overly rigid or inflexible micelles. This rigid micelle structure reduced the system's ability to form a stable nanoemulsion because PEG-40 HCO tended to form lamellar or vesicle structures rather than nanoemulsion droplets. The interface voltage could remain high even if PEG-40 HCO was overused, as there was not enough glycerin as a cosurfactant to degrade the interface energy optimally. This was in contrast to the pseudo-ternary phase diagram of the nanoemulsion formula with an S-mix ratio of 2:3, in which case the lack of PEG-40 HCO reduced the system's ability to form smaller oil droplets, thereby reducing the area of the nanoemulsion (Mai et al., 2018; Alam et al., 2019).

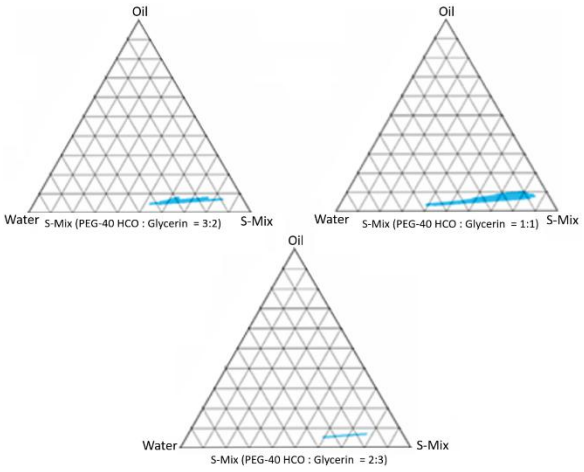

Figure 1. Pseudo-ternary phase diagrams of MSO nanoemulsion formulas with S-mix ratios of 3:2 (A), 1:1 (B), and 2:3 (C).

Meanwhile, the pseudo-ternary phase diagram of the nanoemulsion formula with the S-mix ratio of 1:1 illustrates the most optimal ratio of PEG-40 HCO to glycerin, where the amount of glycerin that was present could loosen the micelle structure and increase the flexibility of the PEG-40 HCO layer around the MSO droplets; the two worked together effectively in lowering the interface tension and creating a more stable structure, enabling the formation of tiny and stable oil droplets to occur. As a result, this ratio produced the most extensive area of nanoemulsion (Ledet et al., 2014).

NE-MO Formulations

Six formulas were applied to make preparations of nanoemulsion with the S-mix ratio

of 1:1, as depicted in the pseudo-terniary diagram. The factor considered in the formula selection was the concentration of MSO. Based on previous research, a nanoemulgel preparation containing 5% moringa oil could provide anti-wrinkle properties (Duraivel et al., 2014). Therefore, in this study, nanoemulsion preparations using 5%, 7%, and 7% MSO were developed, each being varied in oil composition and S-mix, resulting in six formula variations (Table I).

Table I. Optimized nanoemulsion formulas

Formula	Oil/S-mix	% Oil	% S+CoS	% water
NE-MO1	1:12	5.0	60	35
NE-MO1	1:12	5.0	60	35
NE-MO3	1:11	6.0	66	28
NE-MO3	1:11	6.0	66	28
NE-MO4	1:10	6.0	60	34
NE-MO5	1:10	7.0	70	23
NE-MO6	1: 9	7.0	63	30

Characterization of NE-MO and stability

The results of the NE-MO formula characterization test, including the globule size, polydispersity index, and zeta potential after manufacture and after the heating-cooling cycle stability test for as many as six cycles (Table II).

Globule Size

Stable nanoemulsions have small globule sizes and are not readily subject to phase separation. The size of the globules of nanoemulsions ranges from 10 to 100 nm (Dinshaw et al., 2021; Gupta et al., 2016). Before the heating-cooling cycle stability test, the average globule size of the NE-MO formulations ranged from 22.33 nm to 40.02 nm, indicating the achievement of good nanoemulsion formulas, as it was less than 100 nm (Table II). The morphology of the nanoemulsions observed using TEM micrographs (Figure 2a-b). The NE-MO nanodroplets appeared dark, and the surroundings were light and round, with various sizes from 20 nm to 50 nm. The NE-MO globule size was below 100 nm, according to the results of NE-MO globule size measurements.

The order of NE-MO formulas in terms of globule size from the smallest to the largest was NE-MO2, NE-MO1, NE_MO3, NE-MO4, NE-M06, and NE-MO5. After statistical analysis, the globule sizes of NE-MO1, NE-MO2, NE-MO3, and NE-MO4 were not significantly different ($p > 0.05$), and the size of the NE-MO5 globules was the largest.

Based on the test results, it was found that small particle sizes were obtained when the concentration of MSO ranged from 5% to 6%. An increase in the concentration of MSO led to an increase in the size of the globules. This result is in line with the research by Sakeena et al. (2011), which reported that an increase in oil content increased the size of the nanoemulsion globules.

The size of the globules formed in the NE-MO formulas resulted from the equilibrium of MSO, PEG-40 HCO, glycerin, and water. NE-MO5 had the highest concentration of surfactant and the lowest water content, so it had the highest viscosity; this could affect the efficiency of mechanical energy during emulsification, causing the energy distribution for producing tiny droplets to be suboptimal (Alliod et al., 2019). Excessive surfactant concentrations can lead to the formation of micelle structures that disrupt the stability of droplets (Algahtani et al., 2022), while low water concentrations reduce the interaction process between molecules, resulting in large globule sizes (Gupta et al., 2016).

After the heating-cooling cycle stability test, it was found that the globule sizes of NE-MO1 and NE-MO2 did not change significantly compared to the sizes before the test ($p > 0.05$). However, in NE-MO2, the average change in globule size and the standard deviation were smaller, making it reasonable to declare NE-MO2 as the most stable. In contrast, NE-MO3, NE-MO4, NE-MO5, and NE-MO6 showed increases in globule size, especially NE-MO5, which more than doubled (Table II). The equilibrium between MSO, S-mix, and water content in NE-MO2 could minimize changes in globule size, making it the most stable formula. On the other hand, the instability of NE-MO5 was caused by the excessive use of S-mix and the lower water content, which could increase the stiffness of the interface layer and reduce the mobility of the globules, making NE-MO5 more susceptible to coagulation during the thermal cycling test cycle (Harwansh et al., 2019).

Polydispersity Index

The polydispersity index (PDI) is a parameter used to describe the particle size distribution in a system, such as nanoemulsions. Low PDI values indicate relatively uniform particle sizes, while high PDI values indicate more significant particle size variations (Gupta et al., 2016). The PDI values of all NE-MO formulas, with average values ranging from 0 .129 to 0.205 (Table II).

Table II. Nanoemulsion characterization of moringa seed oil

Formula	Before the Heating-Cooling Cycle Stability Test			After the Heating-Cooling Cycle Stability Test		
	Z-average	PDI	Zeta Potential	Z-average	PDI	Zeta Potential
NE-MO1	22.538±0.279	0.129±0.011	-22.57±10.56	26.274±1.425	0.168±0.064	-13.45±3.72
NE-MO2	22.336±0.445	0.175±0.081	-21.14±4.96	22.574±0.447	0.124±0.017	-13.89±0.25
NE-MO3	24.464±1.407[a]	0.137±0.048	-20.00±8.33	47.350±1.894[a]	0.206±0.003	-9.92±0.98
NE-MO4	25.067±0.461[b]	0.145±0.026	-13.73±1.36	28.697±1.044[b]	0.125±0.005	-11.05±2.20
NE-MO5	40.018±1.976[c]	0.205±0.019[e]	-18.56±3.50	114.189±2.609[c]	0.336±0.037e	-12.24±1.43
NE-MO6	27.902±1.163[d]	0.149±0.019	-17.64±2.33[f]	38.988±2.780[d]	0.161±0.010	-11.48±0.76[f]

The same notification shows a significant difference at $\alpha = 0.05$

These results indicate that the NE-MO formulas were relatively mono-dispersive because they were in the value range of 0.1–0.3 (Danaei et al., 2018). The order of NE-MO formulas in terms of PDI from the smallest to the largest was NE-MO1, NE-MO3, NE-MO4, NE-MO6, NE-M02, and NE-MO5. After statistical analysis of globule size, it turned out that there was no significant difference for all formulas ($p > 0.05$).

This uniformity of PDI values of the NE-MO formulas could be attributed to the compatibility between MSO, PEG-40 HCO, glycerin, and water, as well as the speed and duration of stirring during the formulation process. These factors contributed to the relatively uniform formation of globules (Algahtani et al., 2022). Low PDI values provide various advantages, such as increased stability, bioavailability, physical properties, and efficiency of interaction with biological targets, thus positively impacting the overall effectiveness of nanoemulsion formulations (Campolo et al., 2020; Mohammed et al., 2020; Sun et al., 2024).

Based on the results of the heating-cooling cycle stability test, it was found that the PDI value of NE-MO1 increased by 29.9%, the PDI value of NE-MO2 decreased by 29.0%, the PDI value of NE-MO3 increased by 49.8%, the PDI value of NE-MO4 decreased by 13.8%, the PDI value of NE-MO5 increased by 65.84%, and the PDI value of NE-MO6 increased by 8.6%. In conclusion, NE-MO6 was the most stable. However, after statistical analysis, it was found that NE-MO1, NE-MO2, NE-MO3, NE-MO4, and NE-MO6 had PDI values that were not significantly different from the previous values ($p > 0.05$), and only NE-MO5 experienced a significant increase ($p < 0.05$), with a PDI value of more than 0.3, indicating that there was a tendency for nanoemulsion system instability.

Zeta Potential

Zeta potential is a measure of the electrical charge on the surface of colloidal particles and is an important indicator in determining the stability of a dispersion system. This potential describes how much repulsion force the particles in the system have, which affects the colloid system's stability (Lunardi et al., 2021). Zeta potential values in the range of −5 mV to +5 mV indicate the occurrence of rapid aggregation. Meanwhile, values around −20 mV or +20 mV indicate moderate stability. Nanoemulsions that have zeta potential values above +30 mV or below −30 mV are considered stable, and those with excellent stability have zeta potential values higher than +60 mV or lower than −60 mV (Lunardi et al., 2021; Marzuki et al., 2019).

The average zeta potential of the NE-MO formulas was between -13.73 mV and -22.57 mV, which indicates moderate stability (Table II). No formula reached a high stability threshold (±30 mV). The order of the NE-MO formulas in terms of average zeta potential absolute values from the smallest to the largest was NE-MO4, NE-MO6, NE-MO5, NE-MO3, NE-MO2, and NE-MO1. However, statistical analysis revealed that the zeta potential values of all the NE-MO formulas were not significantly different ($p > 0.05$). These results show that the variation in the composition of oil, surfactant, cosurfactant, and water in the NE-MO formulas did not significantly affect the zeta potential obtained. PEG-40 HCO and glycerin were the main components in the S-mix (55–70%) and were likely to dominate in determining the zeta potential. In other words, small changes in the formula composition did not provide significant variations. These results align with previous research by Rachmawati et al. (2017), which used PEG-40 HCO as a surfactant.

As PEG-40 HCO is anonionic surfactant, although not charged, it can produce negative zeta potential values. The mechanism of nonionic surfactants to produce negative zeta potential involves a combination of adsorption of OH^- ions, interaction of polar groups with water, influence of medium pH, and steric effects of surfactant molecular distribution (Ibrahim et al., 2015).

After the heating-cooling cycle stability test, the average absolute value of zeta potential of the NE-MO formulas decreased. The mean decrease in the absolute value of zeta potential of NE-MO1 was -9.11 mV, that of NE-MO2 was -7.25 mV, that of NE-MO3 was -10.08 mV, that of NE-MO4 was -2.68 mV, that of NE-MO5 was -6.32 mV, and that of NE-MO6 was -6.16 mV. From these results, it can be seen that NE-MO4 experienced the least decrease. However, the statistical test results revealed that NE-MO1, NE-MO2, NE-MO3, and NE-MO4 were not significantly different from the previous values ($p > 0.05$). In contrast, NE-MO5 and NE-MO6 experienced significant decreases in zeta potential values ($p < 0.05$).

In general, temperature changes have a meaningful effect on the zeta potential of nanoemulsions. An increase in temperature can decrease the zeta potential value due to increased particle motion and weakened electrostatic interactions. In contrast, lower temperatures stabilize these systems better by maintaining higher zeta potential values and reducing aggregation tendencies (Bhatt et al., 2011; Rahman et al., 2024). However, the zeta potential values of the NE-MO1, NE-MO2, NE-MO3, and NE-MO4 formulas did not change significantly after the stability test. The formulations already had good strength, with a strong stabilizer and consistent load distribution, leading to resistance to stress induced by temperature changes. This study's results align with the research by Khalid et al. (2023), which reported that the increase in temperature did not change the zeta potential value of a vitamin D nanoemulsion enriched with canola oil.

On the other hand, the high oil content in NE-MO5 and NE-MO6 could potentially increase the oil-water interface voltage. The high content of S-mix, especially in NE-MO5, led to oversaturation, thereby decreasing the system's stability due to particle agglomeration. Another contributing factor was the low water content in NE-MO5, which increased the system's viscosity, ultimately affecting the particles' dynamic stability in the nanoemulsion (de Oca-Ávalos et al., 2017).

Morphology

TEM micrographs represent NE-MO on a microscopic scale. The NE-MO nanodroplets appeared dark, while the surroundings were light, spherical in shape, and with size variations from 20 nm to 50 nm (Figure 2a and 2b). The NE-MO globule size range was below 100 nm, meeting the globule size requirements of nanoemulsions (Gupta et al., 2016).

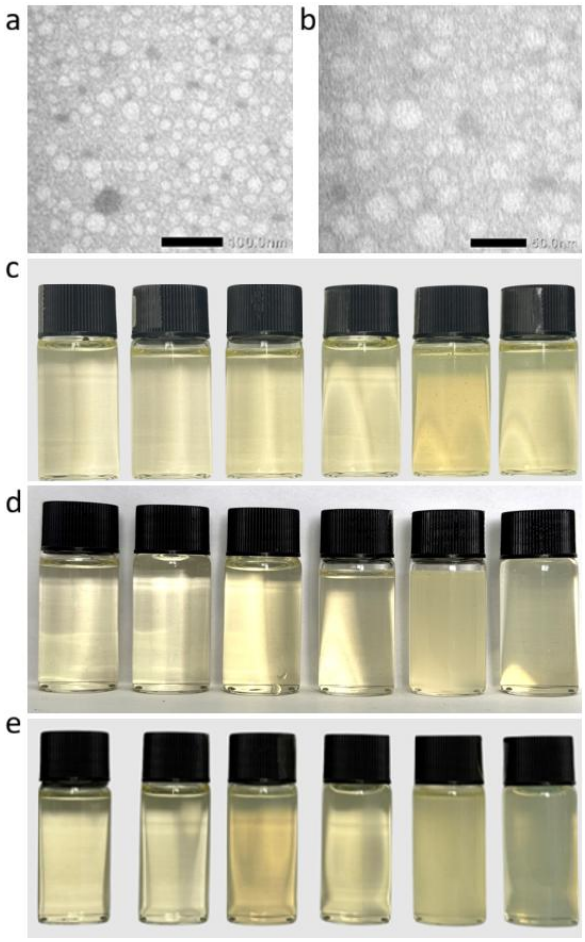

Figure 2. NE-MO TEM displays on the 100 nm (a) and 50 nm (b) scales; the appearance of freshly formulated NE-MO (c), NE-MO stored at room temperature for one month (d), and NE-MO subjected to heating-cooling stability testing (e) is presented sequentially from left to right as NE-MO1, NE-MO2, NE-MO3, NE-MO4, NE-MO5, and NE-MO6.

FTIR analysis results

ATR-FTIR analysis was carried out to test the success of the formation of nanoemulsions. The MSO, PEG-40 HCO, glycerin, and nanoemulsion spectra were recorded at 400–4000 cm^{-1} using an ATR-FTIR spectrometer (Shimadzu, Japan) (Figure 3).

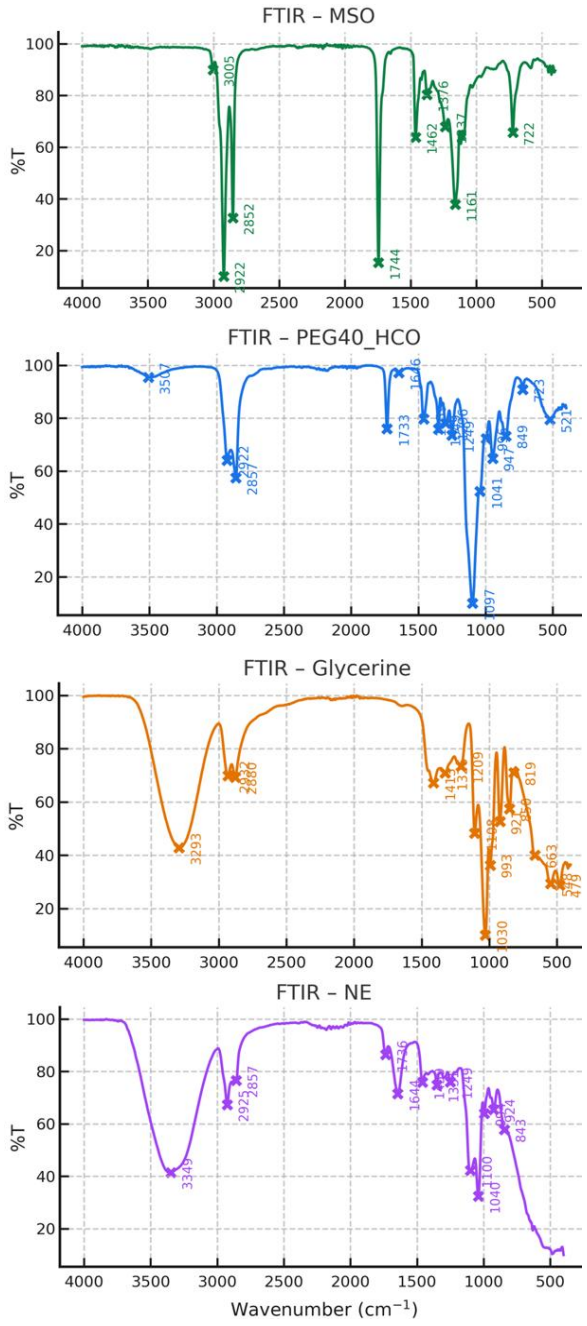

Figure 3. The FTIR spectra from top to bottom are MSO, PEG-40 HCO, Glycerin, and NE-MO mixtures of constituent materials.

The MSO FTIR spectrum had a peak at wave numbers 2922.31 cm^{-1} and 2852 cm^{-1}, which are symmetrical and asymmetrical stretches of the C-H connection in the CH_2 group present in fatty acids, respectively (Bouchareb et al., 2021). The peak at the wave number of 1744 cm^{-1} is caused by the vibrations of the carbonyl group (C=O), indicating the presence of fatty acids in MSO (Bouchareb et al., 2021). The peak at the wave number of 1161 cm^{-1} represents the combined asymmetrical stretching of the (C–C(=O)–O) and (OC–C) bonds (Timilsena et al., 2017). The most intensive peak at the lower end of the spectrum, centred at 722 cm^{-1}, is associated with shaking vibration and out-of-field methylene deformation in the substituted cis olefin (Fu et al., 2021). These results are similar to the research by Irnawati et al. (2024). The PEG-40 HCO spectrum had a weak peak at the wave number of 3507 cm^{-1}, which illustrates the presence of an OH group in the PEG-40 HCO compound. The band has a strong peak at the wave numbers of 2922 cm^{-1} and 2857 cm^{-1}, which are symmetrical and asymmetrical stretches of the C-H connection in the CH_2 group present in PEG 40 HCO, respectively. The peak at the wave number of 1733 cm^{-1} is caused by the vibrations of the carbonyl group (C=O), and the peak at the wave number of 1097 cm^{-1} is a combination of (C–C(=O)–O) and (OC–C) asymmetrical stretches. The peak between 995.50 cm^{-1} and 723 cm^{-1} is an intense stretch of C-H from alkenes (Timilsena et al., 2017; Skoog et al., 2017).

The glycerol FTIR spectrum shows the stretch of OH at 3293 cm^{-1}, while the stretch of CH is indicated by the peak in the region between 2932 cm^{-1} and 2880 cm^{-1}. Bending of the C-O-H group was observed in the area of 1413 cm^{-1}, and stretching of the primary alcohol C-O was observed at the peak of 1108 cm^{-1}. These results are similar to the study by Danish et al. (2017).

The FTIR domains of interest in nanoemulsions are 3600–3100 cm^{-1} (O–H vibration), 3000–2800 cm^{-1} (C–H stretch vibration), and 1800–1600 cm^{-1} (C=O vibration). In the 3600–3100 cm^{-1} range, the relevant band is a large absorption band with a peak at 3349 cm^{-1}, which is associated with O-H stretch vibrations from water molecules, PEG 40 HCO, and glycerin. The symmetrical and asymmetrical stretch vibrations of methylene ($-CH_2$) of the aliphatic chain give rise to absorption bands with peaks at 2925 cm^{-1} and 2857 cm^{-1}. The band with a peak at 1736 cm^{-1} is caused by the vibrations of the carbonyl bonds (C=O) of MSO and PEG 40 HCO. The presence of water molecules produces an absorption band at

1644 cm^{-1}, resulted from the bending vibration of H–O–H (Vasylieva et al., 2018). The absorption band at 1100 cm^{-1} is associated with the asymmetrical stretching of carboxylic acids and esters (Skoog et al., 2017). Finally, the NE-MO FTIR spectra show an insignificant shift in the number of waves and no new peak bands formed, proving that the materials that made up NE-MO were compatible.

The physical stability properties of NE-MO

The results of the physical property test of the six NE-MO formulas include pH, viscosity, and percent transmittance after manufacture and one-month storage at room temperature, as well as after the heating-cooling cycle stability test (Figure 4).

pH test results

The NE-MO which stored for one month at room temperature had an average pH between 6.73 and 7.32 (Figure 4a). The order of NE-MO formulas in terms of pH from the lowest to the highest was NE-MO2, NE-MO1 = NE-MO4 ($p < 0.05$), NE-MO3, NE-MO6, and NE-MO5. Data analysis showed that, after one month of storage at room temperature, each formula had a relatively stable pH ($p > 0.05$). The stability was supported by the inert properties of PEG-40 HCO, a nonionic surfactant with minimal chemical reaction with active ingredients, making pH change less likely. This result aligns with the research by Khalid et al. (2023), which showed that the pH of nanoemulsions did not change during storage at room temperature.

The NE-MO2 formula, which had the lowest S-mix level, showed the lowest pH, while the NE-MO5 formula, which had the highest S-Mix level, had the highest pH. Meanwhile, the NE-MO1 and NE-MO4 formulas, which shared an S-Mix level, showed no meaningful pH difference. This variation in pH between formulas was due to the differences in the concentrations of PEG-40 HCO and glycerin as S-Mix, where the higher the S-Mix level the higher the pH. PEG-40 HCO is known to have a pH ranging from 6 to 7 at specific concentrations. At high concentrations, the interaction between PEG-40 HCO molecules and water can produce hydroxide ions (OH^-) that increase pH. In addition, high concentrations of glycerin can also affect the balance of ions in solution by binding to H^+ ions, thereby increasing the concentration of OH^- , which contributes to the increase in pH (Wulansari & Umarudin, 2020).

The heating-cooling cycle stability test showed consistent results (Figure 4b). None of the NE-MO formulas experienced a statistically significant change in pH. Nanoemulsions formulated with nonionic surfactants such as PEG-40 HCO often show a stable pH after stability tests at various temperatures due to several factors. Nonionic surfactants are chemically stable and have no ionic charge, so they are resistant to pH changes and variations in ionic strength. These surfactants also resist temperature-induced hydrolysis, thereby reducing the formation of by-products that can alter pH (Wulansari & Umarudin, 2020). In addition, NE-MO contains glycerin, which has a natural buffering capacity that helps stabilize pH. The use of deionized or purified water also increases the stability of the system. Characteristics like these make nonionic-surfactant-based nanoemulsions highly resistant to pH fluctuations under thermal stress (Gurpreet & Singh, 2018).

Generally, the NE-MO formulas' pH range was above the skin's natural pH range in the stratum corneum, that is from 4.1 to 5.8 (Proksch, 2018). However, the skin still tolerates this pH range of NE-MO because it was below the safe limit, that is 8 (SNI, 1996). Based on the test results, it is known that the pH of NE-MO2 was the closest to the pH of the skin (6.73).

Viscosity test results

Viscosity measurement is one of the most important parameters in evaluating the quality and physical stability of nanoemulsions (Sharma et al., 2016). The order of preparations from the lowest to the highest in terms of viscosity was NE-MO2, NE-MO1 = NE-MO4 ($p > 0.05$), NE-MO6, NE-MO3, and NE-MO5 (Figure 4c). After one month of storage, the viscosity of NE-MO1, NE-MO2, NE-MO3, NE-MO4, and NE-MO6 did not change ($p > 0.05$). These results prove that nanoemulsions with the right composition have good physical stability, which is in line with the explanation by de Oca-Ávalos et al. (2017). On the other hand, NE-MO5 experienced an increase in viscosity ($p < 0.05$). The occurrence of droplet aggregation in NE-MO5 was a factor causing the increase in viscosity.

The variance in viscosity of the NE-MO formulas was influenced by the concentration of S-mix, which consisted of PEG-40 HCO and glycerin. The formula with the highest S-mix content, NE-MO5 (70%), had the highest viscosity. In contrast, the formula with the lowest S-mix content, NE-MO2 (55%), had the lowest viscosity. Increased concentrations of surfactant and cosurfactant encourage stronger intermolecular interactions and the formation of more complex microstructures. The dense and uniform nanoemulsion structure increases the viscosity (Nuryanti et al., 2018).

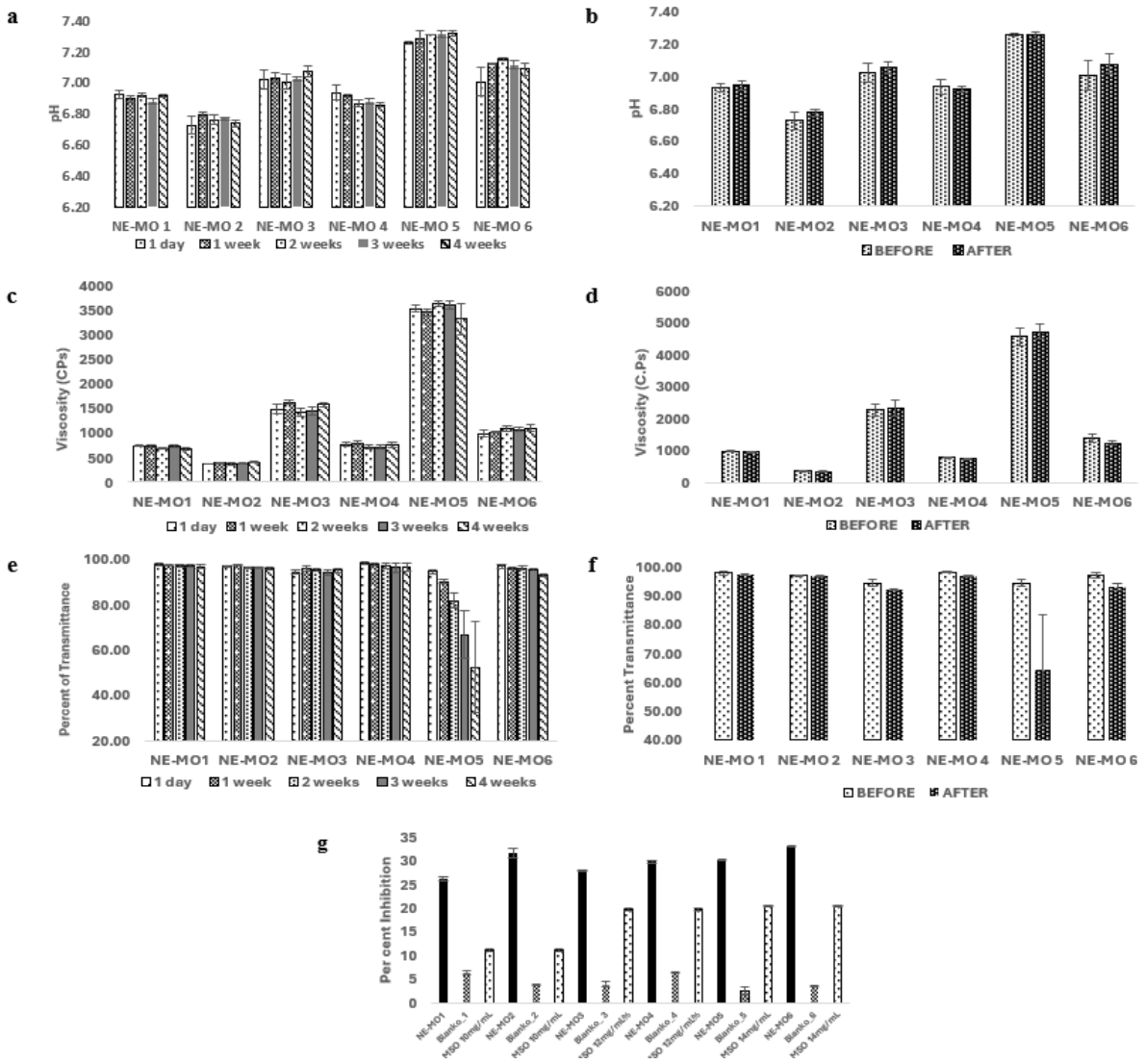

Figure 4. The pH values of the NE-MO formulas after one month of storage at 25°C (a) and a comparison of pH values before and after the heating-cooling cycling test (b); the viscosity of the NE-MO formulas after one month of storage at 25°C (c) and a comparison of viscosity before and after the heating-cooling cycling test (d); the percent transmittance of the NE-MO formulas after one month of storage at 25°C (e) and a comparison of percent transmittance before and after the thermal cycling test (f); the antioxidant activity of NE-MO, NE-MO base, and MSO (g).

The results of the viscosity test of the NE-MO formulations after the heating-cooling cycle stability test showed that the viscosity of NE-MO2 decreased significantly ($p < 0.05$), while the other NE-MO formulas, NE-MO1, NE-MO3, NE-MO4, NE-MO5, and NE-MO6, did not change significantly ($p > 0.05$) (Figure 4d). This study's results align with the research by Alam et al. (2012), which reported that the viscosity of betamethasone nanoemulsions remained stable after stability tests. The decrease in viscosity in NE-MO2 was likely due to the formula's high moisture content and low S-mix content.

Percent transmittance (%T) test results

The percent transmittance (%T) of nanoemulsion formulas is directly related to the clarity of the emulsions. The clarity of a nanoemulsion is determined by the size of the droplets and the emulsion system's homogeneity and stability. Nanoemulsions with a high percent transmittance (close to 100%) have good

transparency, which generally reflects the small size and even distribution of the droplets (Laxmi et al., 2015). Data showed that the percent transmittance of the NE-MO formulas after one month of storage at room temperature, with an average range of 94.40–98.30% (Figure 4c). At the beginning of storage, the order of formulas from the lowest to the highest in terms of percent transmittance was NE-MO3, NE-MO5, NE-MO2, NE-MO6, NE-MO1, and NE-MO4. However, after analysis, it was figured out that the percent transmission of NE-MO1, NE-MO2, NE-MO4, and NE-MO6 did not differ significantly ($p > 0.05$), higher than that of NE-MO3 and NE-MO5, which was not significantly different from each other ($p > 0.05$). All the NE-MO formulas appeared clear (Figure 3c). Furthermore, after one month of storage, it was found that the percent transmittance of NE-MO1 and NE-MO4 was stable ($p > 0.05$), while NE-MO2 and NE-MO3 experienced a slight increase ($p < 0.05$). However, the percent transmittance of NE-MO5 and NE-MO6 decreased ($p < 0.05$), with NE-MO5 especially experiencing a drastic decrease ($p < 0.05$), depicting significant instability. The percent transmittance of NE-MO1, NE-MO2, NE-MO3, NE-MO4, and NE-MO6 was not significantly different ($p > 0.05$). From these results, it was found that NE-MO4 was the best formula because it had the highest and most stable percent transmittance. Despite these percent transmittance findings, the globule size data are still considered more accurate. The appearance of NE-MO formulas after one month of storage were clear except the NE-MO5 is cloudy (Figure 2d).

Formulation factors such as the ratio of oil to S-Mix, oil content, and process parameters (e.g., homogenization conditions) play an important role in determining the stability of nanoemulsions (de Oca-Ávalos et al., 2017). The equilibrium of the composition of MSO, S-Mix, and water in NE-MO1, NE-MO2, NE-MO3, and NE-MO4 resulted in stable percent transmittance over one month of storage at room temperature, as reported by de Oca-Avalos et al. (2017).

The results of the percent transmittance test of the NE-MO formulas after going through the heating-cooling cycle stability test showed that the NE-MO1, NE-MO4 did not change significantly ($p > 0.05$), while NE-MO2, NE-MO3, NE-MO5, and NE-MO6 experienced significant decreases in percent transmittance ($p < 0.05$) (Figure 4f). The decrease in percent transmittance was very sharp, especially in NE-MO5. These results prove that the compositions of NE-MO1, NE-MO2, NE-MO3, NE-MO4, and NE-MO6 were optimal.

The decreases in percent transmittance and turbidity in NE-MO5 after the heating-cooling cycle stability test were likely due to the high concentration of MSO (7%) and S-mix ratio (70%), which increased the risk of droplet coagulation. In addition, the low water phase (23%) reduced the hydration of the surfactant layer. A repeated heating-cooling cycle can damage the stability of an emulsion, leading to greater magnification of droplets and light scattering (Uluata et al., 2016) (Figure 3e).

Thermodynamic stability test results

Centrifugation test

The principle of a centrifugation test is to use centrifugal force to accelerate the separation of components in a NE-MO formula based on the difference in the density of each component (Fitriani et al., 2016). Observations at a centrifugation speed of 5000 rpm for 30 minutes indicated that all freshly prepared NE-MO formulations remained stable, exhibited no phase separation, and retained their clarity. Similarly, NE-MO formulations subjected to heating-cooling stability testing exhibited no phase separation, and NE-MO3 and NE-MO5 were still cloudy.

Antioxidant activity

Examination of the MSO antioxidant activity resulted in an IC_{50} value of 56.64 mg/mL, with vitamin C as a control, which had an IC_{50} value of 1.80 μg/mL. This result shows that the antioxidant activity of MSO was relatively weak. However, this result is better than the study by Athikomkulchai et al. (2021), which obtained an MSO IC_{50} value of 121.9 mg/mL. The order of NE-MO formulas from the lowest to the highest in terms of percent inhibition was NE-MO1, NE-MO3, NE-MO4 = NE-MO5, NE-MO2, and NE-MO6 (ANOVA, $\alpha = 0.05$) (Figure 4g). At the same MSO level, the NE-MO formulas' percent inhibition was higher than that of MSO inhibition. NE-MO has a tiny particle size, which increases the surface area and allows for better dispersion of MSO in methanol solvents; the larger surface area increases interaction between the antioxidant compounds in MSO and DPPH free radicals, thereby increasing antioxidant activity. This study's results align with previous research, which found that the antioxidant activity of nanoemulsion forms is higher than that of pure oil forms (Santos et al., 2021).

CONCLUSION

This study successfully formulated and evaluated MSO nanoemulsions (NE-MO) using PEG-40 HCO as a surfactant and glycerin as a co-surfactant. The pseudo-ternary diagrams created in this study show that the S-Mix ratio of 1:1 was the most optimal composition, resulting in the broadest area of nanoemulsion with a stable droplet structure. Of the six formulas developed, NE-MO2 proved to be the most physically and thermodynamically stable, with the smallest globule size (22.33 nm), showing no significant changes after stability tests. A low PDI value (≤ 0.2) indicates a uniform particle size distribution, while a zeta potential value of -13.73 to -22.57 mV indicates moderate stability.

The NE-MO formulas showed a stable pH in the range of 6.7–7.3, which was still within the safe limit for topical applications. The high percent transmittance (≥ 94%) in most formulas confirms the transparency of the nanoemulsions, while the increased antioxidant activity of NE-MO compared to pure MSO confirms the superiority of nanoemulsions in enhancing bioactivity. The results of the thermodynamic stability test show that the NE-MO formula with a balanced composition of oil, S-Mix, and water could maintain its stability against thermal stress. In contrast, the formula with high concentrations of oil and S-Mix (NE-MO5) had significant instability.

Overall, the NE-MO formula with an S-Mix ratio of 1:1, NE-MO2, is the optimal formula for physically and chemically stable topical applications and has better antioxidant activity potential than pure oils.

ACKNOWLEDGMENTS

The researchers would like to thank the Ministry of Education and Culture of the Republic of Indonesia for funding this research with contract number 181/E5/PG.02.00/2023, as well as Universitas Ahmad Dahlan and Universitas Muhammadiyah Malang for facilitating and helping with this research.

CONFLICT OF INTEREST

The authors declare no conflict of interest.

REFERENCES

Abdelraouf, W., Mattar, A., El-Desouky, S., & Elrefaey, A. (2023). Preparation and characterization nanoemulsion Moringa oil by whey protein and application in ice cream as a food model. *Egyptian Journal of Dairy Science*, *0*(0), 0–0. https://doi.org/10.21608/ejds.2023.207208.1012

Aditya, N. P., Macedo, A. S., Doktorovova, S., Souto, E. B., Kim, S., Chang, P. S., & Ko, S. (2014). Development and evaluation of lipid nanocarriers for quercetin delivery: A comparative study of solid lipid nanoparticles (SLN), nanostructured lipid carriers (NLC), and lipid nanoemulsions (LNE). *Lwt*, *59*(1), 115–121. https://doi.org/10.1016/j.lwt.2014.04.058

Alam, M. S., Baboota, S., Ali, M. S., Ali, M., Alam, N., Alam, M. I., & Ali, J. (2012). Accelerated stability testing of betamethasone dipropionate nanoemulsion. *International Journal of Pharmacy and Pharmaceutical Sciences*, *4*(4), 76–77. https://web.archive.org/web/20180413060812id_/http://ijppsjournal.com/Vol4Suppl4/4483.pdf

Alander, J. T. (2012). Chemical and physical properties of emollients. In M. Lodén & H. I. Maibach (Eds.), *Treatment of dry skin syndrome: the art and science of moisturizers* (Vol. 9783642276, pp. 1–591). Springer. https://doi.org/10.1007/978-3-642-27606-4

Algahtani, M. S., Ahmad, M. Z., & Ahmad, J. (2022). Investigation of factors influencing formation of nanoemulsion by spontaneous emulsification: impact on droplet size, polydispersity index, and stability. *Bioengineering*, *9*(8). https://doi.org/10.3390/bioengineering9080384

Alliod, O., Messager, L., Fessi, H., Dupin, D., & Charcosset, C. (2019). Influence of viscosity for oil-in-water and water-in-oil nanoemulsions production by SPG premix membrane emulsification. *Chemical Engineering Research and Design*, *142*, 87–99. https://doi.org/10.1016/j.cherd.2018.11.027

Athikomkulchai, S., Tunit, P., Tadtong, S., Jantrawut, P., Sommano, S. R., & Chittasupho, C. (2021). Moringa oleifera seed oil formulation physical stability and chemical constituents for enhancing skin hydration and antioxidant activity. *Cosmetics*, *8*(1), 1–18. https://doi.org/10.3390/COSMETICS8010002

Azeem, A., Rizwan, M., Ahmad, F. J., Iqbal, Z., Khar, R. K., Aqil, M., & Talegaonkar, S. (2009).

Nanoemulsion components screening and selection: A technical note. *AAPS PharmSciTech*, *10*(1), 69–76. https://doi.org/10.1208/s12249-008-9178-x

Bhatt, N., Prasad, R. K., Singh, K., & Panpalia, G. . (2011). Stability study od O/W emulsions using zeta potential. *Journal of Chemical and Pharmaceutical Research*, *2*(1), 512–527. https://www.jocpr.com/articles/stability-study-of-ow-emulsions-using-zeta-potential.pdf

Bouchareb, R., Derbal, K., & Benalia, A. (2021). Optimization of active coagulant agent extraction method from Moringa Oleifera seeds for municipal wastewater treatment. *Water Science and Technology*, *84*(2), 393–403. https://doi.org/10.2166/wst.2021.234

Campolo, O., Giunti, G., Laigle, M., Michel, T., & Palmeri, V. (2020). Essential oil-based nano-emulsions: Effect of different surfactants, sonication and plant species on physicochemical characteristics. *Industrial Crops and Products*, *157*. doi.org/10.1016/j.indcrop.2020.112935

Chasanah, U. (2021). Studies on antioxidant activity of red, white, and black pomegranate (Punica granatum L.) peel extract using DPPH radical scavenging method. *Farmasains : Jurnal Farmasi Dan Ilmu Kesehatan*, *5*(2), 51–55. https://doi.org/10.22219/farmasains.v5i2.13472

Danaei, M., Dehghankhold, M., Ataei, S., Hasanzadeh Davarani, F., Javanmard, R., Dokhani, A., Khorasani, S., & Mozafari, M. R. (2018). Impact of particle size and polydispersity index on the clinical applications of lipidic nanocarrier systems. *Pharmaceutics*, *10*(2), 1–17. https://doi.org/10.3390/pharmaceutics10020057

Danish, M., Mumtaz, M. W., Fakhar, M., & Rashid, U. (2017). Response surface methodology based optimized purification of the residual glycerol from biodiesel production process. *Chiang Mai Journal of Science*, *44*(4), 1570–1582. https://epg.science.cmu.ac.th/ejournal/journal-detail.php?id=8483

de Oca-Ávalos, J. M. M., Candal, R. J., & Herrera, M. L. (2017). Nanoemulsions: stability and physical properties. *Current Opinion in Food Science*, *16*, 1–6. https://doi.org/https://doi.org/10.1016/j.cofs.2017.06.003

Dinshaw, I. J., Ahmad, N., Salim, N., & Leo, B. F. (2021). Nanoemulsions: A review on the conceptualization of treatment for psoriasis using a 'green' surfactant with low-energy emulsification method. In *Pharmaceutics* (Vol. 13, Issue 7). doi.org/10.3390/pharmaceutics13071024

Duraivel, S., Shaheda, S. A., Basha, S. R., Pasha, S. E., & Jilani, S. (2014). Formulation and evaluation of antiwrinkle activity of cream and nano emulsion of Moringa oleifera seed oil. *IOSR Journal of Pharmacy and Biological Sciences*, *9*(4), 58–73. https://doi.org/10.9790/3008-09415873

Fitriani, E. W., Imelda, E., Kornelis, C., & Avanti, C. (2016). Karakterisasi dan stabilitas fisik mikroemulsi tipe A / M dengan berbagai fase minyak (Characterisation and phisycal stability of microemulsion type W/O). *Pharmaceutical Sciences and Research*, *3*(1), 31–44. https://scholarhub.ui.ac.id/cgi/viewcontent.cgi?article=1162&context=psr

Fu, X., Su, J., Hou, L., Zhu, P., Hou, Y., Zhang, K., Li, H., Liu, X., Jia, C., & Xu, J. (2021). Physicochemical and thermal characteristics of Moringa oleifera seed oil. *Advanced Composites and Hybrid Materials*, *4*(3), 685–695. https://doi.org/10.1007/s42114-021-00302-4

Gaikwad, M. T., Marathe, R. P., & Pathan, I. B. (2024). The choice of components and the impact of surfactants and co-surfactants on Eplerenon nanoemulsion synthesis for gel-based transdermal application. *International Journal of Applied Pharmaceutics*, *16*(6), 158–168. doi.org/10.22159/ijap.2024v16i6.52044

Gharsallah, K., Rezig, L., Msaada, K., Chalh, A., & Soltani, T. (2021). Chemical compositionand profile characterization of moringa oleifera seed oil. *South African Journal of Botany*, *137*, 475–482. https://doi.org/10.1016/j.sajb.2020.11.014

Gradzielski, M., Duvail, M., De Molina, P. M., Simon, M., Talmon, Y., & Zemb, T. (2021). Using microemulsions: formulation based on knowledge of their mesostructure. *Chemical Reviews*, *121*(10), 5671–5740. https://doi.org/10.1021/acs.chemrev.0c00812

Gupta, A., Eral, H. B., Hatton, T. A., & Doyle, P. S. (2016). Nanoemulsions: formation, properties and applications. *Soft Matter*,

12(11), 2826–2841. https://doi.org/10.1039/c5sm02958a

Harwansh, R. K., Deshmukh, R., & Rahman, M. A. (2019). Nanoemulsion: Promising nanocarrier system for delivery of herbal bioactives. *Journal of Drug Delivery Science and Technology*, *51*, 224–233. https://doi.org/https://doi.org/10.1016/j.jddst.2019.03.006

Ibrahim, N., Raman, I. A., & Yusop, M. R. (2015). Effect of functional group of non-ionic surfactants on thr stability of emulson. *Malaysian Journal of Analytical Sciences*, *19*(1), 261–267. https://mjas.analis.com.my/wp-content/uploads/2018/11/Norsakinah_19_1_31.pdf

Irnawati, Rohman, A., Yamin, Fadzillah, N. A., Azmi, A. A., Nurlatifah, Windarsih, A., Susidarti, R. A., & Ruslin. (2024). Moringa oleifera seed oils: Physico-chemical characterization and its authentication using FTIR spectroscopy and chemometrics. *Case Studies in Chemical and Environmental Engineering*, *10*(October), 100994. https://doi.org/10.1016/j.cscee.2024.100994

K. Gurpreet, & S. K. Singh. (2018). Review of nanoemulsion formulation and characterization techniques. *Indian Journal of Pharmaceutical Sciences*, *80*(5), 781–789. https://doi.org/10.4172/pharmaceutical-sciences.1000422

Khalid, A., Arshad, M. U., Imran, A., Haroon Khalid, S., & Shah, M. A. (2023). Development, stabilization, and characterization of nanoemulsion of vitamin D3-enriched canola oil. *Frontiers in Nutrition*, *10*. https://doi.org/10.3389/fnut.2023.1205200

Kiromah, N. Z. W., Sugihartini, N., & Nurani, L. H. (2023). Development and characterization of clove oil microemulsion. *Pharmacia*, *70*(1), 233–241. https://doi.org/10.3897/pharmacia.70.e98096

Kleiman, R., Ashley, D. A., & Brown, J. H. (2008). Comparison of two seed oils used in cosmetics, moringa and marula. *Industrial Crops and Products*, *28*(3), 361–364. https://doi.org/https://doi.org/10.1016/j.indcrop.2008.04.003

Laxmi, M., Bhardwaj, A., Mehta, S., & Mehta, A. (2015). Development and characterization of nanoemulsion as carrier for the enhancement of bioavailability of artemether. *Artificial Cells, Nanomedicine and Biotechnology*, *43*(5), 334–344. https://doi.org/10.3109/21691401.2014.887018

Ledet, G., Pamujula, S., Walker, V., Simon, S., Richard, G., & Mandal, T. K. (2014). Development and in vitro evaluation of a nanoemulsion for transcutaneous delivery. *Drug Dev Ind Pharm*, *40*(3), 370–379. https://doi.org/10.3109/03639045.2012.763137.

Leone, A., Spada, A., Battezzati, A., Schiraldi, A., Aristil, J., & Bertoli, S. (2016). Moringa oleifera seeds and oil: Characteristics and uses for human health. *International Journal of Molecular Sciences*, *17*(12), 1–14. https://doi.org/10.3390/ijms17122141

Lunardi, C. N., Gomes, A. J., Rocha, F. S., De Tommaso, J., & Patience, G. S. (2021). Experimental methods in chemical engineering: Zeta potential. *Canadian Journal of Chemical Engineering*, *99*(3), 627–639. https://doi.org/10.1002/cjce.23914

Mai, C., Nakorn, A., & Park, I. (2018). Effect of surfactant mixture ratio and concentration on nanoemulsion physical stability. *Thai Journal of Pharmaceutical Sciences*, *42*(supplement), 93–97. http://www.tjps.pharm.chula.ac.th/proceedings/backend/proceeding_file/24_PN_FP_Sukanya Settharaksa (102-106).pdf

Marzuki, N. H. C., Wahab, R. A., & Hamid, M. A. (2019). An overview of nanoemulsion: Concepts of development and cosmeceutical applications. *Biotechnology and Biotechnological Equipment*, *33*(1), 779–797. https://doi.org/10.1080/13102818.2019.1620124

Mohammed, N. K., Muhialdin, B. J., & Meor Hussin, A. S. (2020). Characterization of nanoemulsion of Nigella sativa oil and its application in ice cream. *Food Science and Nutrition*, *8*(6), 2608–2618. https://doi.org/10.1002/fsn3.1500

Montes de Oca-Ávalos, J. M., Candal, R. J., & Herrera, M. L. (2017). Nanoemulsions: stability and physical properties. *Current Opinion in Food Science*, *16*, 1–6. https://doi.org/10.1016/j.cofs.2017.06.003

Nadya, P. F., Choirul, U., Lidya, A., & Dwi, N. (2020). The effect of glycerin as penetration enhancer in a ketoprofen solid preparation-patch on in vitro penetration study through rat skin.

Annals of Tropical Medicine and Public Health, *23*(3), 146–158. https://doi.org/10.36295/ASRO.2020.2338

Nuryanti, N. S. P., Martono, E., Ratna, E. S., & Dadang. (2018). Characteristics and toxicity of nanoemulsion formulation of Piper retrofractum and Tagetes erecta extract mixtures. *Journal of Tropical Plant Pests and Diseases*, *18*(1), 1–11. https://doi.org/10.23960/j.hptt.1181-11

Pegoraro, N. S., Camponogara, C., Cruz, L., & Oliveira, S. M. (2021). Oleic acid exhibits an expressive anti-inflammatory effect in croton oil-induced irritant contact dermatitis without the occurrence of toxicological effects in mice. *Journal of Ethnopharmacology*, *267*(October 2020). https://doi.org/10.1016/j.jep.2020.113486

Proksch, E. (2018). pH in nature, humans and skin. *Journal of Dermatology*, *45*(9), 1044–1052. https://doi.org/10.1111/1346-8138.14489

Purnamawati, S., Indrastuti, N., Danarti, R., & Saefudin, T. (2017). The role of moisturizers in addressing various kinds of dermatitis: A review. *Clinical Medicine and Research*, *15*(3–4), 75–87. https://doi.org/10.3121/cmr.2017.1363

Rachmawati, H., Novel, M. A., Ayu, S., Berlian, G., Tandrasasmita, O. M., Tjandrawinata, R. R., & Anggadiredja, K. (2017). The in vitro–in vivo safety confirmation of PEG-40 hydrogenated castor oil as a surfactant for oral nanoemulsion formulation. *Scientia Pharmaceutica*, *85*(2), 1–10. https://doi.org/10.3390/scipharm85020018

Rahman, A., Mojiono, M., Fansuri, H., Alhamal, B., & Salis, S. (2024). *Nanoemulsion stability of Javanese long pepper extract (Piper retrofractum Vahl): Effects of emulsion system and storage temperature*. *01055*. https://doi.org/10.1051/bioconf/202414601055

Rosyidah, A., Baroroh, E., Annisa, Y., Lestari, S. R., Susanto, H., & Gofur, A. (2024). Efficacy of single love garlic xtract on self nanoemulsifying drug delivery system (SCGE-SNEDDS) on cytokine expression in vitro. *Indonesiam Journal of Pharmacy*, *35*(4), 690–701.

Rowe, R. C., Sheskey, P. J. & Uinn, M. E. (Eds.). (2009). *Handbook of pharmaceutical excipients* (6th ed). Pharmaceutical Press.

Sakeena, M. H. F., Elrashid, S. M., Munavvar, A. S., & Azmin, M. N. (2011). Effects of oil and drug concentrations on droplets size of palm oil esters (POEs) nanoemulsion. *Journal of Oleo Science*, *60*(4), 155–158. https://doi.org/10.5650/jos.60.155

Santa-María, C., López-Enríquez, S., Montserrat-de la Paz, S., Geniz, I., Reyes-Quiroz, M. E., Moreno, M., Palomares, F., Sobrino, F., & Alba, G. (2023). Update on anti-inflammatory molecular mechanisms induced by oleic acid. *Nutrients*, *15*(1), 1–16. https://doi.org/10.3390/nu15010224

Santamarina, A. B., Pisani, L. P., Baker, E. J., Marat, A. D., Valenzuela, C. A., Miles, E. A., & Calder, P. C. (2021). Anti-inflammatory effects of oleic acid and the anthocyanin keracyanin alone and in combination: effects on monocyte and macrophage responses and the NF-κB pathway. *Food & Function*, *12*(17), 7909–7922. https://doi.org/10.1039/D1FO01304A

Santos, D. S., de Moura, L. D., Radicchi, M. A., Azevedo, R. B., Costa, M. C. P., de Souza, P. E. N., Camara, A. L., da Silva, J. R., Muehlmann, L. A., & Longo, J. P. F. (2021). Nanoemulsion improves Babassu palm oil (Orbignya phalerata) antioxidant properties. *Brazilian Archives of Biology and Technology*, *64*, 1–14. https://doi.org/10.1590/1678-4324-2021190387

Sarfaraz Alam, M., Salahuddin Ansari, M., Saraswat, R., & Sharma, P. (2019). Formulation and physical evaluation of glucocorticoid loaded Tea tree oil nanoemulsion: a summarized technical note. *International Journal of Pharmaceutical Sciences and Research*, *11*(9), 4375. https://doi.org/10.13040/IJPSR.0975-8232.11(9).4375-87

Shahbaz, M., Naeem, H., Batool, M., Imran, M., Hussain, M., Mujtaba, A., Alsagaby, S. A., Al Abdulmonem, W., El-Ghorab, A. H., Ghoneim, M. M., Shaker, M. E., Abdelgawad, M. A., & Al Jbawi, E. (2024). Antioxidant, anticancer, and anti-inflammatory potential of Moringa seed and Moringa seed oil: A comprehensive approach. *Food Science and Nutrition*, *February*, 6157–6173. https://doi.org/10.1002/fsn3.4312

Sharma, A. K., Garg, T., Goyal, A. K., & Rath, G. (2016). Role of microemuslsions in advanced drug delivery. *Artificial Cells, Nanomedicine and Biotechnology*, *44*(4), 1177–1185. https://doi.org/10.3109/21691401.2015.1012261

Skoog, D. A., Holler, F. J., & Crouch, S. R. (2017). *Principles of Instrumental Analysis*. Cengage Learning. https://books.google.co.id/books?id=RKxbzgEACAAJ

SNI. (1996). SNI 16-4399-1996: Sediaan Tabir Surya (The dosage form of sunscreen). In *Dewan Standardisasi Nasional* (Vol. 16, Issue 4399, pp. 1–3). Dewan Standardisasi Nasional.

Sun, M. Z., Kim, D. Y., Baek, Y., & Lee, H. G. (2024). The effect of multilayer nanoemulsion on the in vitro digestion and antioxidant activity of β-carotene. *Antioxidants*, *13*(10). https://doi.org/10.3390/antiox13101218

Timilsena, Y. P., Vongsvivut, J., Adhikari, R., & Adhikari, B. (2017). Physicochemical and thermal characteristics of Australian chia seed oil. *Food Chemistry*, *228*, 394–402. https://doi.org/10.1016/j.foodchem.2017.02.021

Tirmiara, N., Reveny, J., & Jansen, Silalahi, J. (2019). Formulation and evaluation of moringa seed oil nanoemulsion gel. Asian Journal of Pharmaceutical Research and Development Open, 7(6), 1–5. https://ajprd.com/index.php/journal/article/view/619

Tunit, P., Chittasupho, C., Sriyakul, K., Tungsuruthai, P., Chakkavittumrong, P., Na-Bangchang, K., & Kietinun, S. (2022). Emulgels containing *Perilla frutescens* seed oil, *Moringa oleifera* seed oil, and mixed seed oil: microemulsion and safety assessment. *Polymers*, *14*(12). https://doi.org/10.3390/polym14122348

Uluata, S., Decker, E. A., & McClements, D. J. (2016). Optimization of nanoemulsion fabrication using microfluidization: Role of surfactant concentration on formation and stability. *Food Biophysics*, *11*(1), 52–59. doi.org/10.1007/s11483-015-9416-1

Vasylieva, A., Doroshenko, I., Vaskivskyi, Y., Chernolevska, Y., & Pogorelov, V. (2018). FTIR study of condensed water structure. *Journal of Molecular Structure*, *1167*, 232–238. https://doi.org/10.1016/j.molstruc.2018.05.002

Ventura, A. C. S. S. B., de Paula, T., Gonçalves, J. P., Soley, B. da S., Cretella, A. B. M., Otuki, M. F., & Cabrini, D. A. (2021). The oil from Moringa oleifera seeds accelerates chronic skin wound healing. *Phytomedicine Plus*, *1*(3), 100099. https://doi.org/https://doi.org/10.1016/j.phyplu.2021.100099

Vibhute, S., Kasture, V., Kasture, S., Kendre, P., Rupnar, S., & Pande, V. (2015). Design and characterization of Moringa oleifera seed oil impregnated antiinflammatory topical micro-dispersion. *Der Pharmacia Lettre*, *7*(3), 7–16.

Wang, W., Cai, Y., Liu, Y., Zhao, Y., Feng, J., & Liu, C. (2017). Microemulsions based on paeonol-menthol eutectic mixture for enhanced transdermal delivery: formulation development and in vitro evaluation. *Artificial Cells, Nanomedicine and Biotechnology*, *45*(6), 1241–1246. https://doi.org/10.1080/21691401.2016.1226178

Winarti, L., Sari, L. O. R. K., Ulfa, E. U., & Samsuri, D. A. (2021). Formulation and antioxidant property of bitter melon seed oil loaded into SNEDDS as a nutraceutical. *Indonesian Journal of Pharmacy*, *32*(3), 385–393. https://doi.org/10.22146/ijp.1334

Wu, K. W., Sweeney, C., Dudhipala, N., Lakhani, P., Chaurasiya, N. D., Tekwani, B. L., & Majumdar, S. (2022). Primaquine loaded solid lipid nanoparticles (SLN), nanostructured lipid carriers (NLC), and Nanoemulsion (NE): Effect of lipid matrix and surfactant on drug entrapment, in vitro release, and ex vivo Hemolysis. *AAPS PharmSciTech*, *23*(1), 1–23. https://doi.org/10.1208/s12249-021-02171-y

Wulansari, S. A., & Umarudin, U. (2020). Pengaruh variasi kombinasi surfaktan non ionik (Span 60 dan Peg-40 HCO) terhadap stabilitas fisik mikroemulsi koenzym Q10 (The effect of variations in the combination of non-ionic surfactants (Span 60 and Peg-40 HCO) on the physical stability of coenzyme Q10 microemulsions). *Jurnal Surya Medika*, *6*(1), 77–83. https://doi.org/10.33084/jsm.v6i1.1534

Xiao, Y., Chen, X., Yang, L., Zhu, X., Zou, L., Meng, F., & Ping, Q. (2013). Preparation and oral bioavailability study of curcuminoid-loaded microemulsion. *Journal of Agricultural and Food Chemistry*, *61*(15), 3654–3660. https://doi.org/10.1021/jf400002x

Zhang, P., Liu, N., Xue, M., Zhang, M., Liu, W., Xu, C., Fan, Y., Meng, Y., Zhang, Q., & Zhou, Y. (2023). Anti-inflammatory and antioxidant properties of β-Sitosterol in copper sulfate-induced inflammation in zebrafish (Danio rerio). *Antioxidants (Basel, Switzerland)*, *12*(2). https://doi.org/10.3390/antiox12020391

.